DOI: 10.5516/NET.2011.43.2.175

〈Technical Note〉

ASSESSMENT OF THE SAFETY OF ULCHIN NUCLEAR POWER PLANT IN THE EVENT OF TSUNAMI USING PARAMETRIC STUDY

JI-YOUNG KIM* and KEUM-SEOK KANG
Korea Electric Power Research Institute
Daejeon, 305-380, Korea
*Corresponding author. E-mail : jykim77@kepri.re.kr

Received May 24, 2010
Accepted for Publication December 06, 2010

Previous evaluations of the safety of the Ulchin Nuclear Power Plant in the event of a tsunami have the shortcoming of uncertainty of the tsunami sources. To address this uncertainty, maximum and minimum wave heights at the intake of Ulchin NPP have been estimated through a parametric study, and then assessment of the safety margin for the intake has been carried out. From the simulation results for the Ulchin NPP site, it can be seen that the coefficient of eddy viscosity considerably affects wave height at the inside of the breakwater. In addition, assessment of the safety margin shows that almost all of the intake water pumps have a safety margin over 2 m, and Ulchin NPP site seems to be safe in the event of a tsunami according to this parametric study, although parts of the CWPs rarely have a margin for the minimum wave height.

KEYWORDS : Safety Assessment, Tsunami, Ulchin NPP, Parametric Study

1. INTRODUCTION

In Korea, all nuclear power plants are located along the coastline in order to secure a sufficient amount of cooling water. More specifically, almost all plants are located on the eastern coast. However, the plate boundary traversing the East Sea and tsunamis from this active fault line can affect the eastern coast of the Korean peninsula. As seen in Figure 1, earthquakes have frequently occurred in the northern area of the West Sea of Japan along this plate boundary, and tsunamis that have occurred in this area have been concentrated in the middle of the eastern coast of Korea near Yamato Rise, which is situated in the central part of the East Sea. In particular, as shown in Figure 2, the tsunamis that occurred in 1983 and 1993 directly hit the eastern coast of Korea. Therefore, the Ulchin Nuclear Power Plant (NPP) site, located in the middle of the eastern coast, can be considered the NPP that is the most vulnerable to tsunamis. Generally, for the safe operation of nuclear power plants, a sea level drop is more serious than a sea level rise. Once the water intake facilities, especially the bell mouth of a pump, are exposed above sea water level, it will lead to the shutdown of a nuclear power plant. Sometimes the inhaled air can result in an abrupt pressure surge within the mechanical cooling water system. Moreover, the essential service water pump (ESWP) is related to the safety of the reactor. For this reason, the variation in the sea level caused by tsunamis should be conservatively and accurately estimated.

In the case of Ulchin NPP, extreme or probable highest and lowest water levels were considered in the design of the ESWP and the circulating water pump (CWP), as shown

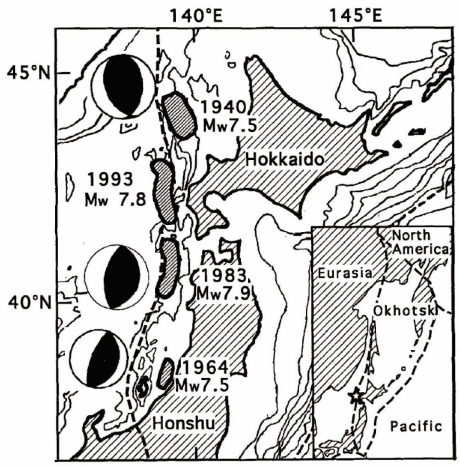

Fig. 1. Source Regions and Focal Mechanisms of Earthquakes Along the Eastern Margin of the East Sea; Plate Boundaries in the Region are Shown in the Inset Map (Satake and Tanioka, 1995 [6])

in Tables 1 and 2. The considered water level included a tide level to the highest water level which was calculated using Shuto's Run-up equation (Shuto, 1972) [1] after calculation of the water level with a linear shallow-water equation on the sea in front of the power plant site. the obtained water depth is up to 200 m under the scenario of a probable maximum earthquake. In the design, the probable maximum tsunami height is regarded as El. 3 m, which is a value estimated through the simplification of coastal landforms without applying numerical models to the power plant site. In addition, wave heights higher than 4 meters have appeared near the nuclear power plant site, as shown in Figure 2, so a revaluation of stability in the event of a tsunami has been continuously required.

In the past, safety assessment of Ulchin NPP site in the event of a tsunami was carried out with probable maximum earthquake magnitude and related tsunami-genic fault parameters (KOPEC, 1986) [2]. Based on the seismic gap theory, since some seismologists warned about earthquakes of larger magnitudes than had been expected, Lee and Lee (2002) [3] evaluated the rise and drop of the sea water level at the intake of Ulchin NPP, based on the fault parameters of the 1983 and 1993 tsunamis and some dangerous faults located in seismic gap area. In addition, Cho et al. (2004) [4] used a combined numerical model based on the shallow water theory to evaluate the wave height changes at the intake of Ulchin NPP resulting from the 1983 tsunami. However, these evaluations did not consider all probable

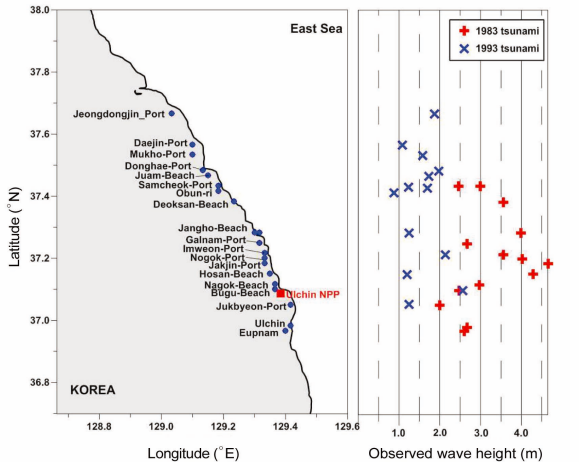

Fig. 2. Maximum Tsunami Height on the Eastern Coast Due to the 1983 and 1993 Tsunamis

Table 1. Specification and Design Extreme Water Level of Ulchin NPP ESWP

Item	Unit 1, 2	Unit 3, 4	Unit 5, 6
Specification	· Pump impeller eye level: El.(-)3.5 m · Main deck level: El.(+)5.5 m · Plant site level: El.(+)10.0 m · Bell mouth level: El.(-)4.7 m	· Bell mouth level: El.(-)6.053 m	· Bell mouth level: El.(-)6.053 m
		· Pump sump bottom level: El.(-)6.51 m · Operating deck level: El.(+)8.12 m · Plant site level: El.(+)10.0 m	
Design extreme water level	· Extreme high water level: El.(+)4.727 m · Extreme low water level: El.(-)1.128 m	· Probable highest water level: El.(+)4.933 m · Probable lowest water level: El.(-)3.300 m	

Table 2. Specification and Design Extreme Water Level of Ulchin NPP CWP

Item	Unit 1, 2	Unit 3, 4	Unit 5, 6
Specification	· Pump impeller eye level: El.(-)1.3 m · Main deck level: El.(+)5.5 m · Plant site level: El.(+)10.0 m · Bell mouth level: El.(-)1.65 m	· Pump sump bottom level: El.(-)7.793 m · Bell mouth level: El.(-)6.662 m	· Pump sump bottom level: El.(-)8.174 m · Bell mouth level: El.(-)7.034 m
		· Operating deck level: El.(+)8.12 m · Plant site level: El.(+)10.0 m	
Design extreme water level	· Extreme high water level: El.(+)4.727 m · Extreme low water level: El.(-)1.128 m	· Probable highest water level: El.(+)4.933 m · Probable lowest water level: El.(-)3.300 m	

tsunami-genic faults, and the tsunami sources are uncertain. In response to this uncertainty, JSCE (2002) [5] suggested a tsunami assessment method for nuclear power plants in Japan which considers the uncertainty of tsunami sources by a parametric study. In this study, maximum and minimum wave heights at the intake of Ulchin NPP were estimated through a parametric study, and an assessment of the safety margin for the intake was carried out.

2. NUMERICAL SIMULATION OF TSUNAMI

2.1 Numerical Models

A far-field tsunami is an event with a propagation distance over 1000 km, and a mesh size from several kilometers to several tens of kilometers is used in this kind of analysis in order to cover the large target area. In this case, the wavelength of a far-field tsunami (several hundreds of kilometers) is larger than the water depth (several kilometers), and its wave height is smaller (several meters). Therefore, nonlinearity can be avoided, and the far-field tsunami analysis code is based on the linear Boussinesq theory. The following governing equations are given in the spherical coordinate system with its origin at the center of the earth because the far-field tsunami is a large-scale phenomenon:

$$\frac{\partial \zeta}{\partial t} = -\frac{1}{a\cos\varphi}\left\{\frac{\partial M}{\partial \lambda} + \frac{\partial}{\partial \varphi}(N\cos\varphi)\right\}, \tag{1}$$

$$\frac{\partial M}{\partial t} = -\frac{gh}{a\cos\varphi}\frac{\partial \zeta}{\partial \lambda} + fN + \frac{1}{a}\frac{\partial}{\partial \lambda}\left(\frac{h^3}{3}F'\right), \tag{2}$$

$$\frac{\partial N}{\partial t} = -\frac{gh}{a}\frac{\partial \zeta}{\partial \varphi} - fM + \frac{1}{a\cos\varphi}\frac{\partial}{\partial \varphi}\left(\frac{h^3}{3}F'\right), \tag{3}$$

$$F' = \frac{1}{a\cos\varphi}\left(\frac{\partial^2(u\cos\varphi)}{\partial t\partial \lambda} + \frac{\partial^2 v}{\partial t\partial \varphi}\right), \tag{4}$$

where M is the discharge flux in the λ-direction (m^2/sec), N is the discharge flux in the φ-direction (m^2/sec), t is time (sec), g is the gravitational acceleration (m/sec^2), h is the still water depth (m), ζ is the water level (m), f is the Coriolis factor (= $2\omega\sin\varphi$), λ is the longitude (rad), φ is the latitude (rad), a is the semi-major axis of the Earth, u is the velocity in the λ-direction (m/sec), and v is the velocity in the φ-direction (m/sec).

On the other hand, a near-field tsunami is an event caused by an earthquake that occurs in a coastal area. Its target area is comparatively small, and can be analyzed with a mesh size ranging from several meters to several kilometers. To delineate bathymetry in a coastal area in detail, the mesh size is normally changed to make it larger in the open sea and smaller in the coastal area. Near-field tsunami analysis code is based on the nonlinear shallow water theory shown in the following equations in order to take into account the abrupt changes of water depth that are characteristic to coastal areas and the topography along the shore. The following governing equations are given in the Cartesian coordinate system:

$$\frac{\partial \zeta}{\partial t} = -\frac{\partial M}{\partial x} - \frac{\partial N}{\partial y} + \frac{\partial \eta}{\partial t}, \tag{5}$$

$$\frac{\partial M}{\partial t} = -g(h+\zeta)\frac{\partial \zeta}{\partial x} - \frac{\partial}{\partial x}\left(\frac{M^2}{h+\zeta}\right) - \frac{\partial}{\partial y}\left(\frac{MN}{h+\zeta}\right) + \nu_H\left(\frac{\partial^2 M}{\partial x^2} + \frac{\partial^2 M}{\partial y^2}\right) - \gamma_b{}^2\frac{M\sqrt{M^2+N^2}}{h+\zeta}, \tag{6}$$

$$\frac{\partial N}{\partial t} = -g(h+\zeta)\frac{\partial \zeta}{\partial y} - \frac{\partial}{\partial x}\left(\frac{MN}{h+\zeta}\right) - \frac{\partial}{\partial y}\left(\frac{N^2}{h+\zeta}\right) + \nu_H\left(\frac{\partial^2 N}{\partial x^2} + \frac{\partial^2 N}{\partial y^2}\right) - \gamma_b{}^2\frac{N\sqrt{M^2+N^2}}{h+\zeta}, \tag{7}$$

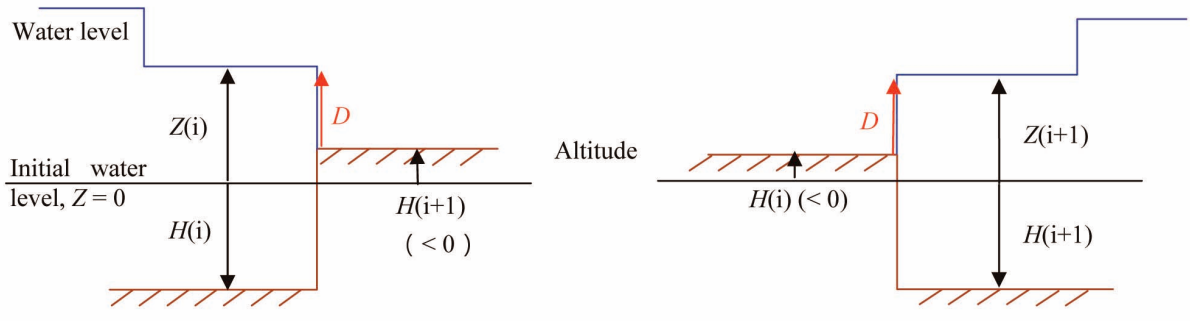

(1) Case from I to I+1 $D = Z(i) + H(i+1)$ (2) Case from I+1 to I $D = Z(i+1) + H(i)$)

Fig. 3. Methods for Analysis of Run-up

where M is the discharge flux in the x-direction (m^2/sec), N is the discharge flux in the y-direction (m^2/sec), ν_H is the horizontal eddy viscosity (m^2/sec), γ_b^2 is the bottom friction ($m^{-1/3}$·sec), η is the bottom deformation (m), h is the still water depth (m), and ζ is the water level (m).

The run-up of a tsunami onto the land can be simulated through nonlinear calculation of the near-field tsunami code. First, the code calculates a D-value, which is the difference between the water level at the front of the running-up tsunami and the altitude of its adjacent mesh. Second, it calculates the discharge flux by substituting the D-value into the equation of motion.

Both far-field and near-field tsunami analysis codes adopt the finite difference method. The codes apply the central difference to the space derivative and the central difference (the leap-frog method) to the time derivative. Numerical analysis of tsunamis requires that the target area be divided into square meshes, and that variables be defined at each mesh as shown in Figure 4 and equations (8) to (10):

$$\frac{\zeta_{i,j}^{n+1/2}-\zeta_{i,j}^{n-1/2}}{\Delta t}+\frac{M_{i+1/2,j}^{n}-M_{i-1/2,j}^{n}}{\Delta x}+\frac{N_{i,j+1/2}^{n}-N_{i,j-1/2}^{n}}{\Delta y}=0 \quad (8)$$

$$\frac{M_{i+1/2,j}^{n+1}-M_{i+1/2,j}^{n}}{\Delta t}+gh\frac{\zeta_{i+1,j}^{n+1/2}-\zeta_{i,j}^{n+1/2}}{\Delta x}=0, \quad (9)$$

$$\frac{N_{i,j+1/2}^{n+1}-N_{i,j+1/2}^{n}}{\Delta t}+gh\frac{\zeta_{i,j+1}^{n+1/2}-\zeta_{i,j}^{n+1/2}}{\Delta y}=0. \quad (10)$$

Near-field tsunami analysis code can seamlessly calculate from large-meshed areas to small-meshed areas as shown in Figure 5. However, the mesh size can change only by 1/2 or 1/3 at the boundary of large and small meshes as shown in Figure 6.

2.2 Simulation Conditions

As there is no observation data of tsunamis at Ulchin NPP site, simulation results for historical tsunamis have been compared with the tidal records of the Mukho tide gauge to verify the simulation results for the East Sea. Analysis of tsunami propagation for the whole East Sea is required because tsunami sources are located in the eastern margin of the East Sea. The mesh areas consist of 6 steps for the Mukho site and 7 steps for the Ulchin NPP site as

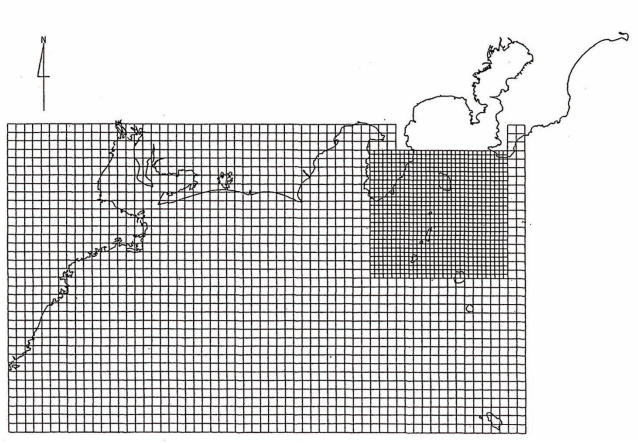

Fig. 5. Example of Mesh Size Change

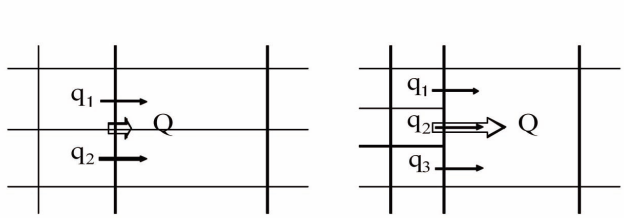

Fig. 6. Method of Continuation of Regions

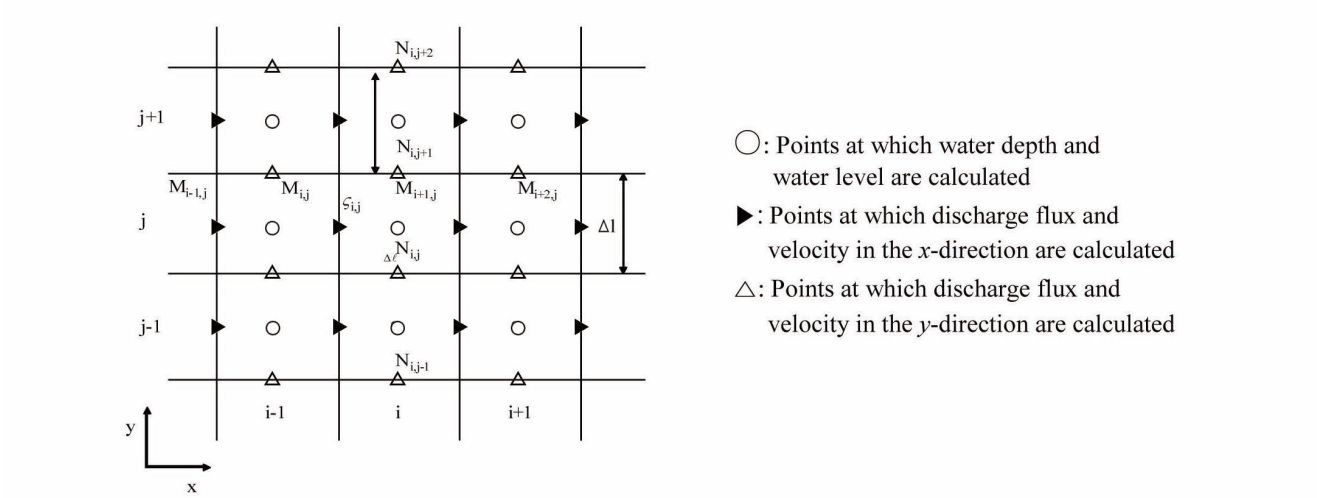

Fig. 4. Mesh and Points at which Variables are Defined

shown in Figure 7 and Table 3. Equations (1) to (4) of far-field analysis code are applied to area 1, and equations (5)-(7) of near-field analysis code are applied to other areas. In Figures 7(a) to 7(c), nested grids are constructed by dynamic linking in the boxed areas. While previous studies applied a grid interval of 1 or 2 minutes for the entire East Sea, this study adopts a grid interval of 2 minutes because it also uses global bathymetric data of 2-minute-interval resolution to set the largest grid zone. When a grid interval decreases by one-third, the smallest mesh size is

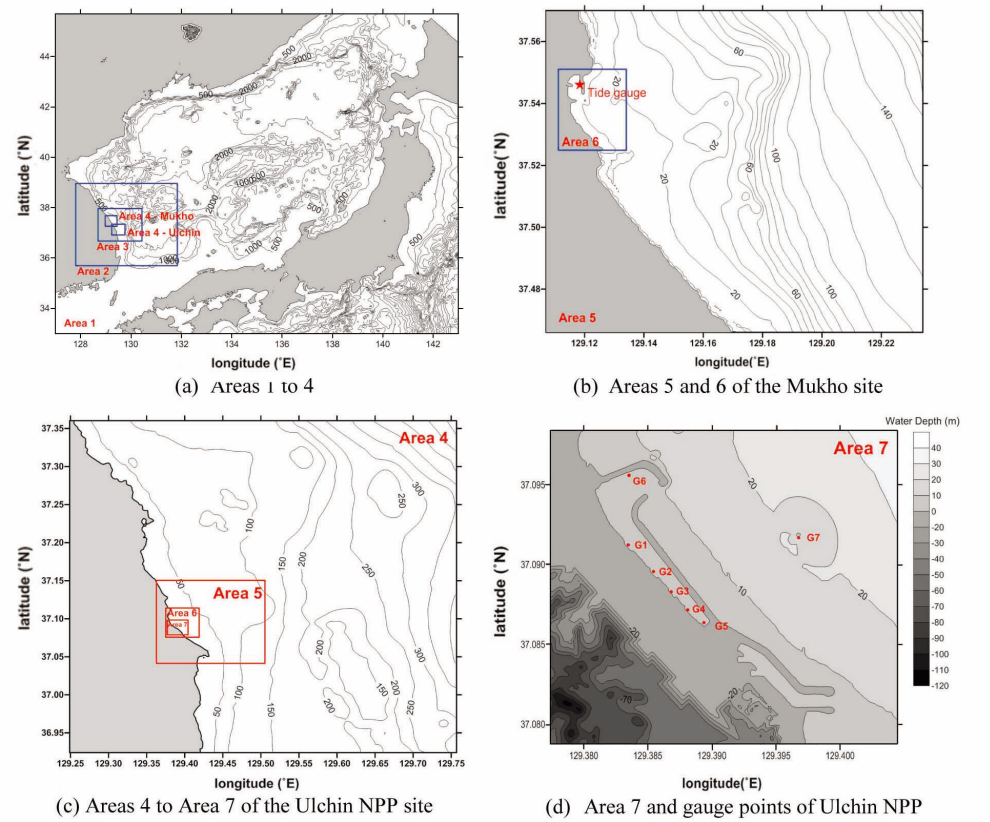

(a) Areas 1 to 4 (b) Areas 5 and 6 of the Mukho site

(c) Areas 4 to Area 7 of the Ulchin NPP site (d) Area 7 and gauge points of Ulchin NPP

Fig. 7. Computational Domains, Bathymetry and Gauge Points

Table 3. Mesh Conditions

Area	Mesh number		Mesh size (m)	Remarks
1	480 × 377		2 minute (≒ 3700 m)	Far-field
2	326 × 337		1100.0	NLSWE
3	421 × 396		370.0	NLSWE
4	Mukho harbor	351 × 394	123.3	NLSWE
4	Ulchin NPP	360 × 388	123.3	NLSWE
5	Mukho harbor	276 × 285	41.1	NLSWE
5	Ulchin NPP	303 × 289	41.1	NLSWE
6	Mukho harbor	149 × 221	13.7	NLSWE
6	Ulchin NPP	281 × 306	13.7	NLSWE
7	Ulchin NPP	521 × 469	4.6	NLSWE

Note: NLSWE is nonlinear shallow water equation

13.7 m for the Mukho site. For the Ulchin NPP site, the width inside of the breakwater is quite narrow, that is, less than 100 m. Therefore, the smallest interval is set as 4.6 m in order to review the wave height in detail. The locations of wave gauge points are shown in Figure 7(d), and points G1 to G5 correspond to the locations of intake water pumps.

2.3 Verification of Simulation Results

Figure 8 shows the results of a comparison between tidal records and simulations of the 1983 and 1993 tsunamis at Mukho harbor. It can be seen that the simulation results are not bad, although the wave period is slightly different. Figure 9 shows the results of a comparison of a simulation

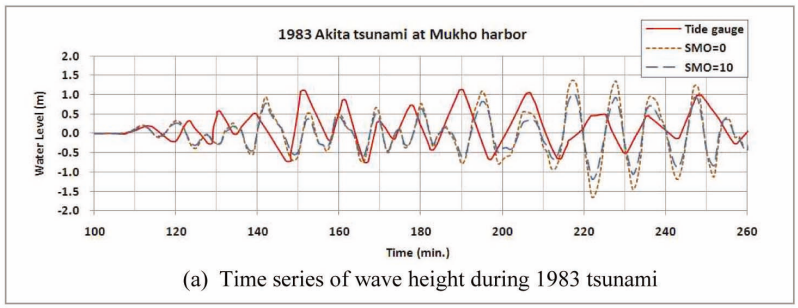

(a) Time series of wave height during 1983 tsunami

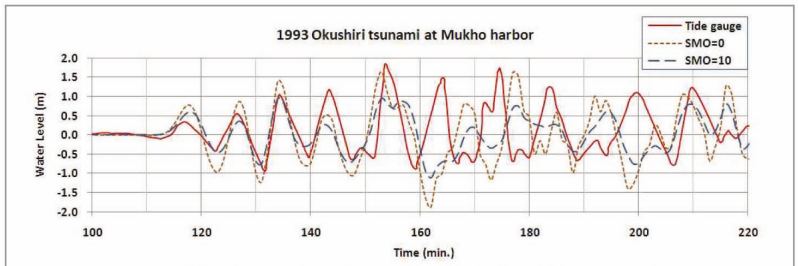

(b) Time series of wave height during 1993 tsunami

Fig. 8. Comparison of Simulation Results with Historical Tsunami Records at Mukho Site

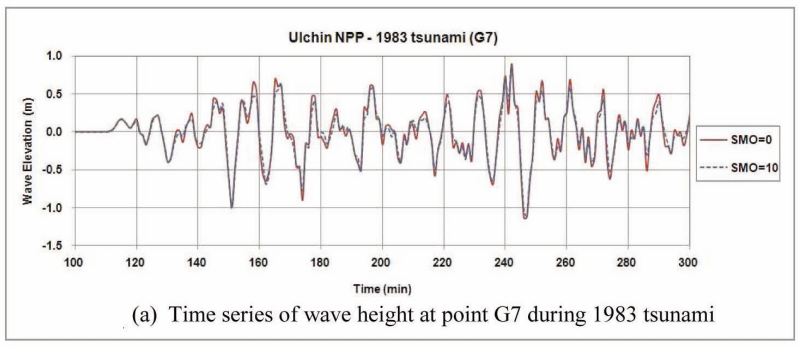

(a) Time series of wave height at point G7 during 1983 tsunami

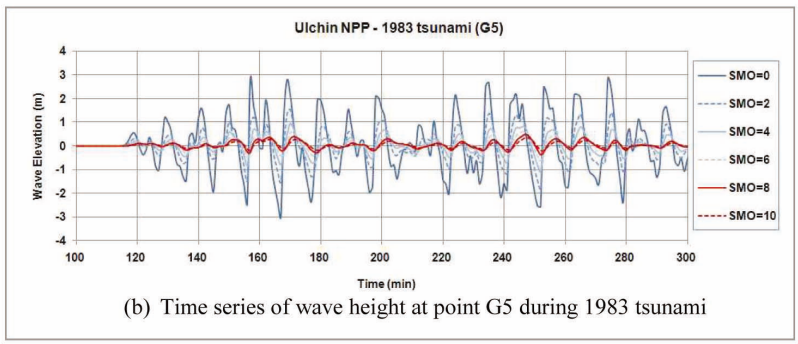

(b) Time series of wave height at point G5 during 1983 tsunami

Fig. 9. Comparison of Simulation Results with Various SMOs at Ulchin Site

of the 1983 tsunami using various coefficients of eddy viscosity. In this model, two parameters need to be calibrated. One is the coefficient of Manning friction, and the other is the coefficient of eddy viscosity. Both cases of Mukho and Ulchin are not sensitive to the former coefficient, and 0.025 $m^{-1/3}$·s has been used. On the other hand, it is found that the latter coefficient considerably affects wave height at the inside of the breakwater of Ulchin NPP as shown in Figure 9(b). For reference, "SMO" is the variable name of the coefficient of eddy viscosity in this model. According to the previous study results in JSCE (2002) [5], when the coefficient of eddy viscosity is 10 m^2/s, the increased length of the highest water level decreases by 5% to 10% in comparison with the coefficient of 0. Furthermore, when the coefficient is 100 m^2/s, the increased length of the highest water level dramatically decreases. That is, if the coefficient of eddy viscosity is smaller than 10 m^2/s, its coefficient hardly affects the wave height and flow patterns, and thus does not need to be considered. However, the influence of this coefficient cannot be ignored for the Ulchin NPP site. It is necessary to select an appropriate value, but there is no observation data of historical tsunamis at the Ulchin NPP site, so verification of simulation results and selection of appropriate coefficients are difficult. For the Mukho site, the effect of the eddy viscosity coefficient is not considerable, and it is hard to determine the best result as shown in Figure 8. From these facts, the effect of eddy viscosity seems to be due to the geometry of the Ulchin NPP intake channel, and detailed investigations of the influence of eddy viscosity and optimal coefficient are required in the future. In this study, a coefficient of 0 is used for conservative assessment because it gives the highest wave. As shown in Figure 10, it seems that the result from the case of a large coefficient is unreasonable because wave calming inside the breakwater occurs when a short period wind wave is coming. However, in the case of a long wave such as a tsunami, the wave height inside the breakwater is amplified commonly.

3. SAFETY ASSESSMENT

3.1 Configuration of Parametric Study

A parametric study is a method of taking into account the uncertainties of tsunami sources in the design, and it is defined as a study in which a large number of numerical calculations are carried out under various conditions. The conditions of a scenario earthquake are set based on a standard fault model, and are varied within an appropriate range. A parametric study should be carried out concerning the dominant factors of the standard fault model. Subsequently, a parametric study of subordinate factors should be carried out by using the fault model determined to be the most effective for the target site. To set up the scenario tsunamis for the parametric study, the fault model of the eastern margin of the East Sea was considered according to JSCE (2002) [5] as shown in Figure 11 and Table 4. Table 5 shows the established standard fault model. In this study, the parametric study was carried out on the factors of fault position, strike angle, and dip angle with the established standard fault model, and it was performed in three stages. In setting a standard fault model of the eastern margin of the East Sea, JSCE (2002) [5] supposed that *d*, which refers to the depth of the upper edge of the fault plane, is 0. This study also fixes the value as 0 because

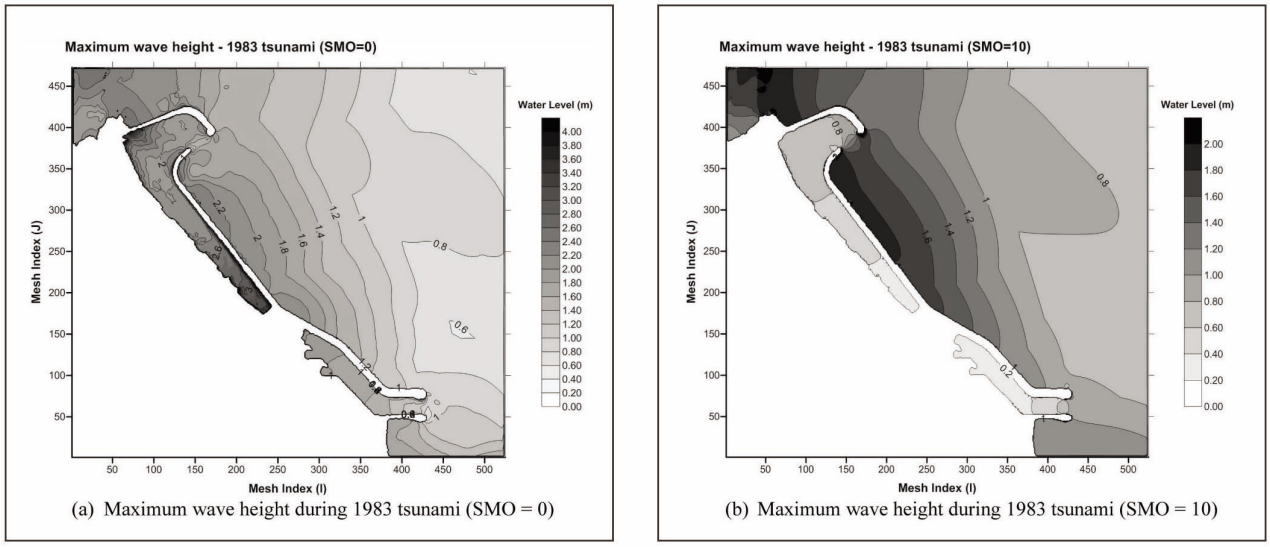

(a) Maximum wave height during 1983 tsunami (SMO = 0)

(b) Maximum wave height during 1983 tsunami (SMO = 10)

Fig. 10. Comparison Between Different SMOs at Ulchin Site

the value has little influence on the change of the highest water level compared to other factors. In the scenario tsunami set above, each stage is organized in consideration of the order of factors of which the sensitivity is greatest, as suggested in JSCE (2002) [5]. The possibility of the fault model causing the biggest change of water level in the target site being selected is set in a greatest way to reduce the number of cases for an efficient calculation. Of course, this scenario tsunami does not include all the possible fault models, and it also has the limitation that it could possibly omit the fault model that shows the biggest change of water level. Recently, research has been conducted to address these limitations, but this study makes the most use of the JSCE method, which has been applied and verified in many countries.

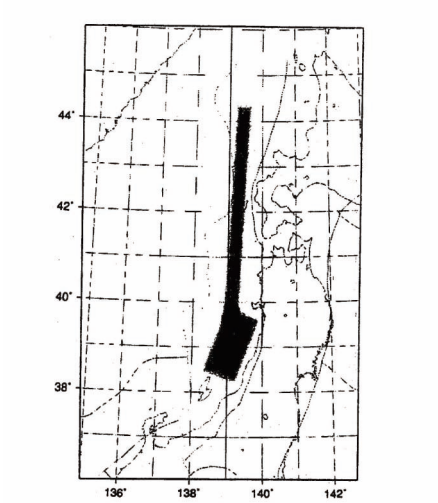

Fig. 11. Location of the Active Fault Area (JSCE, 2002 [5])

The established scenario tsunamis are summarized in Table 6. First, simulations are performed for five cases of stage I as shown in Table 7 and Figure 12, and then, based on the results of stage I, the most severe case which gives the highest and lowest wave at the target site is selected. Subsequently, the strike angle of the selected case is parameterized to four cases, and the most severe case is also selected in stage II. Finally, the dip angle is parameterized in stage III.

3.2 Results of Parametric Study

3.2.1 Stage I: Position of Fault

Simulation results of five cases are given in Table 8. Maximum and minimum tsunami heights in Table 8 were obtained inside the breakwater. From these results, case 3 was selected as the most severe case, which gave a maximum wave height of 3.45 m as shown in Table 8. It is found that the fault of case 3, which is the closest fault to the 1983 tsunami fault, causes the largest wave at the Ulchin NPP site. Meanwhile, the maximum wave height of case 4 is lower than the one given in case 3 because the propagation route of the wave is affected by the Yamato Rise. Arrival times were observed from 110 to 130 minutes after earthquake and were found to depend on the propagation route, such as the distance between coast and fault, so case 1 takes the longest time to arrive.

Table 4. Parameters of the Standard Fault Model (JSCE, 2002 [5])

Sea area	Types of earthquakes	Parameters					
		Fault position	Depth of upper edge of the fault plane (d)	Strike angle (θ)	Dip angle (δ)	Dip direction	Slip angle (λ)
Eastern margin of the East Sea	Earthquakes that occur within the upper crest	○	○	○	○	○ west dip east dip	fixed at 90°

Note: ○ is an item that should be taken into consideration in a 'parametric study'.

Table 5. Established Standard Fault Model

Case	M_w	L (km)	W (km)	M_0 (N·m)	μ (N/m^2)	U (m)	δ (°E)	d (km)	λ (°)
Standard Fault	7.85	131.1	30	7.50E+20	3.50E+10	5.45	30	0	90

Note: M_w is magnitude of earthquake, L is length of fault, W is width of fault, M_0 is moment of earthquake, μ is shear modulus, and U is dislocation depth of fault.

3.2.2 Stage II: Strike Angle

In this stage, the strike angle of case 3 was parameterized as Table 9, and the simulation results of four cases are given in Table 10. Strike angle hardly affects the initial wave height, but it affects the propagation route of the wave. From these results, case 3-3 was selected as the most severe case which gives the highest wave of 4.01 m. If the lowest wave is considered, case 3-4 is more severe than case 3-3. Therefore, it is necessary to consider case 3-4 and case 3-3 together. It can be seen that the influence of case 3-3 and 3-4 is strong because the strike angles of these cases are parallel to the coastline of the Ulchin site.

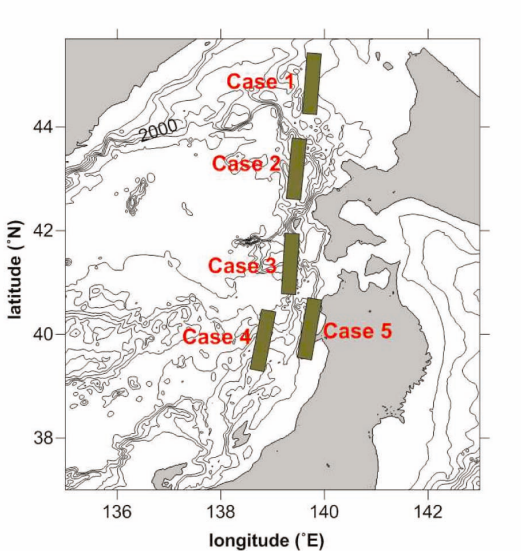

Fig. 12. Fault Locations for Stage I of Parametric Study

3.2.3 Stage III: Dip angle

The dip angles of cases 3-3 and 3-4 were parameterized in stage III as shown in Table 11, and the simulation results of six cases are shown in Table 12. In these results, case 3-3-3 shows the highest wave height of 4.78 m, but the lowest height is not lower than the lowest heights of case 3-3 and case 3-4. Dip angle affects the initial wave height, so the maximum wave heights of case 3-3-1 and 3-3-3 are larger than those of case 3-3 and 3-3-2. Finally, the highest wave height can be obtained from case 3-3-3 because the dip direction is west, and the fault location is closer than case 3-3-1. The results of the case 3-4 series are similar to those of the case 3-3 series, and the lowest wave height was obtained from case 3-4.

3.3 Assessment of Safety Margin

The maximum wave height of case 3-3-3 and the minimum wave height of case 3-4 have been considered in order to assess the safety margin for the intake water pumps. The wave height distributions of these cases are shown in Figure 13, and the highest wave height appears

Table 6. Established Scenario Tsunamis

Stage	Parameter	Value
Stage I	Fault position (5 case)	Described in Table 7
Stage II	Strike angle (4 case)	$\theta \pm 5°$, $\theta \pm 10°$,
Stage III	Dip angle (3 case)	(30°E), 60°E, 30°W, 60°W

Table 8. Simulation Result of Stage I

Case	Tsunami Height (m)		Tsunami Height (m)		Remarks
	Max	Min	Mouth of Breakwater	Inside of Breakwater	
1	2.10	-1.79	127.9	130.5	
2	2.28	-2.25	117.3	119.8	
3	**3.45**	**-2.71**	114.5	117.0	○
4	3.13	-2.70	109.7	112.0	
5	2.99	-2.24	121.2	123.7	

Table 7. Case List of Stage I

Case	Lat. (°N)	Lon. (°E)	M_W	L (km)	W (km)	θ (°E)	U (m)	δ (°E)	d (km)	λ (°)
1	44.2	139.6	7.85	131.1	30	4.3	5.45	30	0	90
2	42.6	139.3	7.85	131.1	30	5.1	5.45	30	0	90
3	40.8	139.2	7.85	131.1	30	3.6	5.45	30	0	90
4	39.4	138.6	7.85	131.1	30	11	5.45	30	0	90
5	39.6	139.5	7.85	131.1	30	10.7	5.45	30	0	90

Table 9. Case List of Stage II

Case	Lat. (°N)	Lon. (°E)	M_w	L (km)	W (km)	θ (°E)	U (m)	δ (°E)	d (km)	λ (°)
Basis (3)	40.8	139.2	7.85	131.1	30	3.6	5.45	30	0	90
3-1	40.8	139.2	7.85	131.1	30	8.6	5.45	30	0	90
3-2	40.8	139.2	7.85	131.1	30	13.6	5.45	30	0	90
3-3	40.8	139.2	7.85	131.1	30	358.6	5.45	30	0	90
3-4	40.8	139.2	7.85	131.1	30	353.6	5.45	30	0	90

Table 10. Simulation Result of Stage II

Case	Tsunami Height (m)		Arrival Time (min)		Remarks
	Max	Min	Mouth of Breakwater	Inside of Breakwater	
Basis (3)	3.45	-2.71	114.5	117.0	
3-1	3.55	-2.28	114.8	117.3	
3-2	3.11	-2.29	115.0	117.5	
3-3	**4.01**	-2.78	114.3	116.8	○
3-4	3.63	**-2.88**	113.6	116.1	○

Table 12. Simulation Result of Stage III

Case	Tsunami Height (m)		Arrival Time (min)		Remarks
	Max	Min	Mouth of Breakwater	Inside of Breakwater	
Basis (3-3)	4.01	-2.78	114.3	116.8	
3-3-1	4.49	-2.47	111.2	113.5	
3-3-2	4.30	-2.67	109.7	112.0	
3-3-3	**4.78**	-2.70	111.0	113.4	○
Basis (3-4)	3.63	**-2.88**	113.6	116.1	○
3-4-1	3.95	-2.69	110.6	113.0	
3-4-2	4.03	-2.77	109.1	111.5	
3-4-3	4.42	-2.81	110.4	112.8	

Table 11. Case List of Stage III

Case	Lat. (°N)	Lon. (°E)	M_w	L (km)	W (km)	θ (°E)	U (m)	δ (°E)	d (km)	λ (°)
Basis (3-3)	40.8	139.2	7.85	131.1	30	358.6	5.45	30	0	90
3-3-1	40.8	139.2	7.85	131.1	30	358.6	5.45	60	0	90
3-3-2	40.8	139.2	7.85	131.1	30	358.6	5.45	150	0	90
3-3-3	40.8	139.2	7.85	131.1	30	358.6	5.45	120	0	90
Basis (3-4)	40.8	139.2	7.85	131.1	30	353.6	5.45	30	0	90
3-4-1	40.8	139.2	7.85	131.1	30	353.6	5.45	60	0	90
3-4-2	40.8	139.2	7.85	131.1	30	353.6	5.45	150	0	90
3-4-3	40.8	139.2	7.85	131.1	30	353.6	5.45	120	0	90

at the innermost point of the inside of the breakwater. Meanwhile, the lowest wave height appears near the mouth of the breakwater, but only the minimum wave height inside the breakwater has been considered in this parametric study. The maximum and minimum wave heights are, as shown in Table 13, at each gauge point that corresponds to the location of each intake water pump. The assessment of the safety margin for the normal

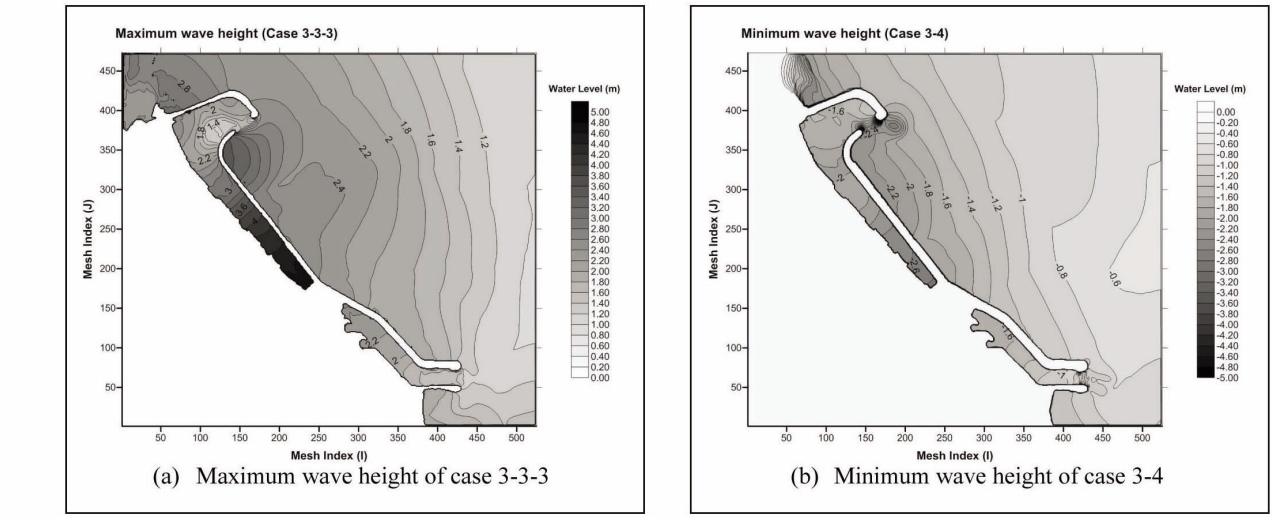

(a) Maximum wave height of case 3-3-3 (b) Minimum wave height of case 3-4

Fig. 13. Maximum and Minimum Wave Height Distributions

Table 13. Maximum and Minimum Wave Heights at Each Gauge Point (unit: m)

Gauge point	G1	G2	G3	G4	G5
Water pump	#1,2 ESWP & CWP	#3,4 ESWP & CWP	#5,6 ESWP	#5 CWP	#6 CWP
Maximum wave height of case 3-3-3	2.85	3.93	4.33	4.58	4.71
Minimum wave height of case 3-4	-1.94	-2.20	-2.55	-2.64	-2.82

Note: ESWP is essential service water pump, CWP is circulating water pump

Table 14. Assessment of Safety Margin at Each Intake Water Pump (unit: m)

		plant site	ESWP			CWP			
			#1,2	#3,4	#5,6	#1,2	#3,4	#5	#6
Run-up	(a) Deck level - HHWL	9.08	4.58	7.20	7.20	4.58	7.20	7.20	7.20
	(b) Maximum wave height	4.78	2.85	3.93	4.33	2.85	3.93	4.58	4.71
	(c) Safety margin (a-b)	4.30	1.73	3.27	2.87	1.73	3.27	2.62	2.49
Run-down	(d) Bell mouth El. - LLWL		-4.37	-5.73	-5.63	-4.47	-6.33	-6.71	-6.71
	(e) NPSH El. * - LLWL	-	-4.10	-4.20	-4.33	-3.90	-2.22	-3.56	-3.55
	(f) Minimum wave height	-	-1.94	-2.20	-2.55	-1.94	-2.20	-2.64	-2.82
	(g) Safety margin for bell mouth (f-d)		2.43	3.53	3.08	2.53	4.13	4.07	3.89
	(h) Safety margin for NPSH (f-e)	-	2.16	2.00	1.78	1.96	0.02	0.92	0.73

Note: * NPSH El. is the required lowest water level considering the net positive suction head of the water pump, HHWL is the highest high-water level, and LLWL is the lowest low-water level

operation of the intake water pumps is shown in Table 14. It can be seen that almost all of the intake water pumps have a safety margin over 2 m. Although parts of CWPs rarely have the margin of net positive suction head (NPSH) for the minimum wave height, ESWPs have a safety margin over 2 m. In conclusion, the Ulchin NPP site seems to be safe in the event of a tsunami, according to this parametric study.

4. CONCLUSION

In this study, the results of tsunami simulation were first verified with the Mukho tidal records for historical tsunamis. Next, the maximum and minimum wave heights at the intake of Ulchin NPP were estimated through a parametric study, and an assessment of the safety margin for the intake was carried out. From the simulation results for the Ulchin NPP site, it can be seen that the coefficient of eddy viscosity considerably affects wave height at the inside of breakwater, because the harbor mouth is so narrow. There is no observation data of historical tsunamis at the Ulchin NPP site, so verification of the simulation result and selection of an appropriate coefficient of eddy viscosity have not been performed in this study. However, it is necessary to investigate the influence of eddy viscosity and the optimal coefficient in a future study. The assessment for safety margin found that almost all of the intake water pumps have a safety margin over 2 m, and the Ulchin NPP site seems to be safe in the event of a tsunami, although parts of the CWPs rarely have a margin for the minimum wave height. Not all scenario tsunamis have been considered in this parametric study, and in fact, there is a limit to how many tsunami scenarios can be considered. Therefore, it is necessary to assess the tsunami hazard risk using a probabilistic method in a future study.

ACKNOWLEDGEMENTS

This study has been supported by IAEA Extrabudgetary Project on the Protection of Nuclear Power Plants against Tsunamis and post Earthquake Considerations in the External Zone.

REFERENCES

[1] Shuto, N., "Standing waves in front of a sloping dike," Coastal Eng. In Japan, Vol. 15, pp. 13-23 (1972).

[2] KOPEC, "Investigation and review for design maximum flood level of KNU 9 & 10 – review of influence of tsunami," Korea Power Engineering Company (1986). (in Korean)

[3] Haegyun Lee and Dae-Soo Lee, "Revaluation of Tsunami Risk at the site of Ulchin Nuclear Power Plant," *Journal of Korean society of coastal and ocean engineers*, Vol. 14, No. 1, pp. 1-7 (2002). (in Korean)

[4] Yong-Sik Cho, So-Beom Jin and Ho-Jun Lee, "Safety analysis of Ulchin Nuclear Power Plant against Nihonkai-Chubu Earthquake Tsunami," *Nuclear engineering and design: an international journal devoted to the thermal, mechanical and structural problems of nuclear energy*, Vol. 228, No. 1/3, pp. 393-400 (2004).

[5] JSCE, "Tsunami Assessment Method for Nuclear Power Plants in Japan," Japan Society of Civil Engineers (2002).

[6] Kenji Satake and Yuichiro Tanioka, "Tsunami Generation of the 1993 Hokkaido Nansei-Oki Earthquake," Journal of Pure and Applied Geophysics, Vol. 145, No. 3/4, pp. 803-821 (1995).